



Remediation of soil polluted with herbicides by Fenton-like reaction: Kinetic model of diuron degradation

Juana M^a Rosas*, Fernando Vicente, Elena G. Saguillo, Aurora Santos, Arturo Romero

Dpto Ingeniería Química, Facultad de Ciencias Químicas, Universidad Complutense Madrid, Ciudad Universitaria S/N, 28040 Madrid, Spain

ARTICLE INFO

Article history:

Received 11 April 2013

Received in revised form 18 June 2013

Accepted 1 July 2013

Available online 12 July 2013

Keywords:

Diuron

Trisodium citrate

Kinetic model

Modified-fenton

Soil remediation

ABSTRACT

Catalytic diuron degradation in soil by modified Fenton or Fenton-like reaction has been studied and a kinetic model including the rates of all physical and chemical processes involved in both aqueous and soil phases has been developed and validated.

The soil selected, a sandy clay loam one, was artificially spiked with a solution of diuron dissolved in methanol, obtaining a final diuron concentration of 0.167 mmol kg⁻¹. Diuron oxidation experiments were performed in a batch reactor in both aqueous phase and slurry system at different concentrations of H₂O₂, trisodium citrate (CT) as chelant, and Fe(III) as catalyst.

Because of the neutral pH achieved by adding CT, the oxidation rate of CT and H₂O₂ decomposition in the aqueous phase has been found negligible. On the contrary, a significant unproductive decomposition of H₂O₂ by the soil was observed. Diuron oxidation rate was strongly dependent on the iron concentration and, in lower extent, on the H₂O₂ concentration, in both aqueous phase and slurry system.

A kinetic model, including diuron desorption, CT adsorption, H₂O₂ decomposition by soil, and diuron oxidation in both soil and aqueous phase was proposed. The kinetic parameters were obtained by fitting the experimental data to this model. The predicted values of diuron abatement, in both soil and aqueous phases, and the H₂O₂ simulated conversion values were in good agreement with the experimental ones. Moreover, the obtained results suggest that kinetic of diuron desorption to the aqueous phase was enhanced due to the chemical reaction.

© 2013 Elsevier B.V. All rights reserved.

1. Introduction

Herbicides are the most extensively type of pesticides used in agriculture. Among them, haloaromatic herbicides are considered a persistent class of chemicals [1]. Diuron (N'-(3,4-dichlorophenyl)-N,N-dimethylurea) is an herbicide, belonging to the phenylamide family and the subclass of phenylurea, used to control a wide variety of annual and perennial broadleaf and grassy weeds. This compound is also used on many agricultural crops such as fruit, cotton, sugar cane, alfalfa and wheat, but is more widely applied for long-term pre-emergence weed control in non-crop areas [2,3]. It is relatively persistent in soil, with half-lives from 1 month to 1 year [4]. Its persistence in soil is due to a combination of three properties: chemical stability, low water solubility and strong adsorption to soil particles [5]. Agricultural use of herbicides results in relatively low soil contamination (diffuse contamination). However, in places where production or storage activities are carried out, a high concentration of these herbicides can be found in the soil caused by spillage, loading and rinsing operations or direct dumping into

soil disposal sites. These practices may be responsible for approximately 45% of cases of ground water contamination [6,7].

In situ chemical oxidation (ISCO) by Fenton's reagent seems to be a viable technology for the remediation of contaminated soils by pesticides [7–9]. In this technique, a strong chemical oxidant is injected into the contaminated surface to destroy the targeted contaminants [10]. Among the oxidants employed in ISCO, the Fenton's reaction is widely used for the remediation of contaminated soil and groundwater, with a large number of in situ applications [11–13]. In order to solve the acid pH requirement of the classical Fenton process, chelating agents can be used in a modified Fenton or Fenton-like reaction [14,15].

In spite of the big potential of Fenton's reagent for soil remediation, few works have focused in the assessment of a kinetic model for contaminants abatement in the aqueous-soil system. And they do not consider separately in the kinetic the solid and aqueous contaminant concentration [16,17]. On the contrary, a large number of kinetic studies have been carried out on Fenton reactions in aqueous solution [18,19].

Besides of the assumed mechanism in aqueous solution, the particular features of the soil presence (desorption, surface reactions, diffusion, etc.) should be taken into account [20]. It has been usually considered that the mechanism of Fenton-like reactions

* Corresponding author. Tel.: +34 91 394 41 71; fax: +34 91 394 41 71.

E-mail addresses: jmrosas@quim.ucm.es, nanirosas@yahoo.es (J.M. Rosas).

Nomenclature

<i>b</i>	constant that relates the apparent kinetic constant of diuron desorption with CT concentration (mol m^{-3}) $^{-1}$
C_{CT}	trisodium citrate 2-hydrate (CT) concentration in aqueous phase (mol m^{-3})
C_D	diuron concentration in aqueous phase (mol m^{-3})
C_{De}	diuron concentration in aqueous phase at the equilibrium stage (mol m^{-3})
$C_{Fe\ aq}$	Fe(III) concentration in aqueous phase (mol m^{-3})
$C_{Fe\ aqe}$	Fe(III) concentration in aqueous phase at the equilibrium stage (mol m^{-3})
$C_{H_2O_2}$	H_2O_2 concentration in aqueous phase (mol m^{-3})
k_{aD}	kinetic constant of diuron adsorption (h^{-1})
k'_{aD}	apparent kinetic constant of diuron adsorption (h^{-1})
k_{Daq}	kinetic constant of diuron oxidation in aqueous phase ($\text{h}^{-1} \text{ mol}^{-1.5} (\text{m}^{-3})^{-1.5}$)
k'_D	apparent kinetic constant of diuron oxidation in aqueous phase (h^{-1})
K_{FD}	Freundlich constant of the diuron sorption isotherm ($(\text{kg}^{-1})(\text{mol})^{0.6} (\text{m}^{-3})^{-0.4}$)
K_{FCT}	Freundlich constant of the CT sorption isotherm ($(\text{kg}^{-1})(\text{mol})^{-0.2} (\text{m}^{-3})^{-1.2}$)
K_{Fe}	equilibrium constant that relates Fe extraction with CT concentration (mol m^{-3}) $^{0.53}$
$k_{H_2O_2}$	kinetic constant of H_2O_2 decomposition rate in soil phase ($\text{m}^3 \text{ kg}^{-1} \text{ h}^{-1}$)
$k_{oxDs\ h}$	kinetic constant of diuron oxidation in soil phase catalyzed by iron in solution ($\text{h}^{-1}(\text{mol m}^{-3})^{-1.8}$)
$k_{oxDs\ H}$	kinetic constant of diuron oxidation in soil phase catalyzed by metals in soil ($\text{h}^{-1}(\text{mol m}^{-3})^{-0.8}$)
n_o	adjustable order of H_2O_2 concentration on diuron oxidation rate
n_1	Freundlich exponent of the diuron sorption isotherm
n_2	Freundlich exponent of the CT sorption isotherm
n_3	exponent that relates Fe extraction as a function of CT concentration
n_4	exponent that takes into account the effect of the H_2O_2 concentration on the diuron oxidation rate in soil phase
n_D	total moles of diuron (mol)
n_{Daq}	total moles of diuron in the aqueous phase (mol)
n_{Ds}	total moles of diuron in the soil phase (mol)
q_{CTe}	CT concentration in soil phase at the equilibrium stage (mol kg^{-1})
q_D	diuron concentration in soil phase (mol kg^{-1})
q_{De}	diuron concentration in soil phase at the equilibrium stage (mol kg^{-1})
X_{Daq}	diuron conversion in aqueous phase
$r_{ads\ D}$	adsorption rate of diuron from the aqueous phase ($\text{mol kg}^{-1} \text{ h}^{-1}$)
$r_{ox\ CTaq}$	oxidation rate of CT in aqueous phase ($\text{mol m}^{-3} \text{ h}^{-1}$)
$r_{dec\ H_2O_2\ aq}$	decomposition rate of H_2O_2 in aqueous phase ($\text{mol m}^{-3} \text{ h}^{-1}$)
$r_{dec\ H_2O_2\ s}$	decomposition rate of H_2O_2 in soil phase ($\text{mol kg}^{-1} \text{ h}^{-1}$)
$r_{ox\ Daq}$	oxidation rate of diuron in aqueous phase ($\text{mol m}^{-3} \text{ h}^{-1}$)
Sg^{BET}	apparent surface area ($\text{m}^2 \text{ g}^{-1}$)
V_L	liquid volume (m^3)
W	soil mass (kg)

takes mainly place through contaminant solubilization from soil to the aqueous phase with further oxidation in the liquid phase. Furthermore, Watts et al. [21] reported that under vigorous modified Fenton conditions, the system owns a greater activity than the standard Fenton's system, due to an enhancement of the contaminant desorption [21,22]. However, other works also consider the possibility of a heterogeneous oxidation of the pollutant at the solid surface [13,23,24].

The main objective of this paper is to establish a kinetic model for diuron degradation in soil, considering the rates of the main physical and chemical processes involved in both aqueous and soil phases. With this goal, different experiments will be carried out in both aqueous phase and slurry system. The model should be able to predict adequately the hydrogen peroxide decomposition and the diuron abatement in both phases. To do this, contributions to oxidation in aqueous and soil phases will be explicitly taken into account in the model and the influence of catalyst (iron) will be also included as an explicit variable. A proper chelating agent selected elsewhere [7] has been also used in order to keep the iron in solution at neutral pH.

Besides, in order to analyze if enhanced desorption by chemical reaction occurs, the kinetic of diuron adsorption will be evaluated in absence and presence of pollutant oxidation.

2. Materials and methods

2.1. Reagents

Reagents of analytical grade were used in the experiments. Diuron 98% and trisodium citrate 2-hydrate (CT) were purchased from Sigma-Aldrich. Hydrogen peroxide 30% (w/w) was provided from Riedel de Haen. Ferric chloride hexahydrate obtained from Fluka was used as the catalytic Fe(III) specie. Potassium permanganate and sulphuric acid 95–98% from Panreac were used in the determination of H_2O_2 . Methanol used as solvent and acetonitrile for mobile phase in HPLC were obtained from Scharlab. Naphthalene >99% from Sigma-Aldrich was used as internal standard in HPLC measurements. All of the suspensions and solutions were prepared with Milli-Q water (>18 MΩ cm) purified with a deionizing system.

2.2. Characterization of soil sample

The soil selected for this study (SE) was categorized as sandy clay loam at natural neutral pH. The properties of the soil sample are listed in Table 1. The measurements of the properties were performed in triplicate to obtain an average value. The soil selected corresponded to subsurface horizon (*E*) at an agriculture zone characterized by the low organic carbon content.

The pH was measured with a pH electrode (Basic 20-CRISON) in 1:2.5 soil/water suspensions. The soil organic matter (SOM) content was determined by incineration of a known weight of sample placed in a ceramic crucible in an electric muffle for 3 h at 823 K, obtaining the corresponding SOM content by mass difference (NEN 5754 Method) [25].

Soil contains two different forms of carbon: Total Organic Carbon (TOC) and Inorganic Carbon (IC). Total carbon (TC) of the soil was determined by using a TOC analyser, as described in the standard procedure EN 13137. Firstly, the sample was divided into two subsamples and one sub-sample was oxidized with an oxygen stream ($0.5 \times 10^{-3} \text{ m}^3 \text{ min}^{-1}$) by using a TOC analyser (TOC-V CSH Shimadzu) with a solid state module (SSM-5000A) at 900 °C and the formed CO_2 was analyzed by non-dispersive infrared absorbance (NDIR). The second sub-sample was pre-treated with 4 mL of concentrated H_3PO_4 to remove the inorganic carbon (IC) and take

Table 1
Soil properties.

Soil	pH	SOM (%)	TC (%)	TOC (%)	IC (%)	Mn (mg g ⁻¹)	Fe (mg g ⁻¹)	Sg ^{BET} (m ² g ⁻¹)
SE	7.2 ± 0.1	0.443 ± 0.021	0.246 ± 0.011	0.246 ± 0.011	–	0.21 ± 0.01	8.3 ± 0.6	4 ± 1

measurement at 473 K. This carbon dioxide is detected by the NDIR and the sample IC concentration is measured in the same way as TC. The IC is a combination of carbonate and bicarbonate. The TOC concentration is determined by difference.

Total Fe and Mn content in soils were determined by acid extraction/atomic absorption spectroscopy (EPA 3050B Method) [26]. The porous structure of the samples was characterized by N₂ adsorption–desorption at 77 K, performed in a SA 3100 surface area analyzer (Coulter). Samples were previously outgassed for at least 8 h at room temperature to avoid soil degradation. From the N₂ isotherm, the apparent surface area (Sg^{BET}) was determined by applying the BET Eq.

2.3. Aqueous phase experiments

H₂O₂ decomposition and diuron and CT degradation in the liquid phase were studied in duplicate through batch experiments. Runs were performed in 500 mL glass vials, kept in continuous agitation. The temperature was controlled and remained at 293 K and the soil pH was not adjusted. Different experiments were carried out by using an initial diuron concentration of 0.086 mol m⁻³, varying CT concentrations from 5 to 50 mol m⁻³, H₂O₂ concentrations from 294 to 1765 mol m⁻³, and Fe(III) concentrations from 0 to 5 mol m⁻³.

2.4. Slurry phase experiments

2.4.1. Contaminated soil

Contaminated soil was artificially prepared by using uncontaminated control soil. The soil was spiked with a solution of diuron dissolved in methanol, the initial concentration of diuron was 0.172 mol m⁻³. Then, the mixture was completely stirred and blended to ensure homogeneity at 293 K for about 72 h with a $V_L \times W^{-1} = 1 \times 10^{-3}$ m³ kg⁻¹. Finally, the mixture was evaporated by a rotary evaporator at 303–308 K, obtaining a homogeneous concentration of 1.7×10^{-4} mol kg⁻¹ of diuron in the spiked soil.

The total remaining amount of the contaminant sorbed in the soil was verified by Soxhlet extraction by using a mixture of dichloromethane/hexane (1:1) as solvents. The amount of total extracted diuron was determined by HPLC.

2.4.2. Adsorption–desorption experiments

All adsorption–desorption experiments of the contaminated soil were performed by using the batch equilibration technique at 293 K. Liquid to solid ratios were varied between 1×10^{-3} to 5×10^{-3} m³ kg⁻¹ when desorption with pure water was evaluated, meanwhile CT concentrations between 0.5 and 50 mol m⁻³ at a fixed $V_L \times W^{-1} = 2 \times 10^{-3}$ m³ kg⁻¹ were also used to analyze both the diuron and Fe desorption with CT from the soil, and the own adsorption of CT into the soil. Duplicate tests were performed for each experiment and the average value was used for figures with an experimental error lower than 5%.

2.4.3. Modified Fenton experiments

Runs were performed in 20 mL glass vials, kept in continuous agitation (50 rpm) on a shaking water bath, supplied by Selecta. The temperature was controlled and remained at 293 K and the soil pH was not adjusted. The liquid phase volume to contaminated soil weight ratio ($V_L \times W^{-1}$) was 2×10^{-3} m³ kg⁻¹. The samples were

collected at different reaction times and immediately centrifuged for 5 min at 5000 rpm in a Centrolit Selecta centrifuge. The supernatant was analyzed for CT, diuron and H₂O₂, as described in the Analytical methods section. Each reaction vial represents one time point and all reactions were conducted in duplicate. In order to avoid possible explosions, due to gas accumulation in the vials, the caps were not sealed during reaction time to permit evacuation of the generated gas. The soil and aqueous phase were separated before the extraction. After centrifugation, the supernatant and soil extracts by Soxhlet extraction method previously explained were analyzed to determine residual diuron concentration by means of HPLC.

Soil samples (1 g) were put in contact with 2 mL of CT or complex iron/citrate solution about 24 h prior to the addition of H₂O₂. Then, H₂O₂ solution was added in an adequate amount to provide the desired concentration. The modified Fenton reaction was just started upon addition of H₂O₂. The different experiments were carried out by using an initial diuron and CT concentration of 1.7×10^{-4} mol kg⁻¹ and 50 mol m⁻³, respectively. H₂O₂ concentrations were varied from 294 to 1765 mol m⁻³, and Fe(III) concentrations from 0 to 5 mol m⁻³. Duplicate tests were performed for each experiment and the average value was used for figures with an experimental error lower than 5%.

2.5. Analytical methods

In order to determine the residual diuron concentration and the presence or not of some aromatic degradation products with the reaction time, 20 μL of sample was injected into a high-performance liquid chromatography column. The initial concentration of the substrate and its transformation was monitored by HPLC (Agilent, mod. 1100). A Poroshell 120 SB-C18 2.7 μm Performance column (100–4.6 mm) was used as the stationary phase. The mobile phase was acetonitrile–water (40:60, v/v) with a flow-rate of 10^{-6} m³ min⁻¹. The detection and quantification of diuron was carried out by an Agilent 1290 Infinity Diode Array Detector. The effluent was monitored at 210 nm.

The concentration of H₂O₂ in solution was determined by titration with a solution of potassium permanganate, KMnO₄, of known concentration, in sulphuric acid by using a potentiometric titration analyzer supplied by Metrohm.

Ion chromatography was used to determine citrate concentration with an anion chromatography column (Metrosep A Supp 5-250/40, Metrohm) and a mobile phase containing a buffer (HCO₃²⁻/CO₃²⁻) and an acid suppressor.

Soluble iron concentrations were analyzed by using a DR/890 colorimeter with the FerroVer Iron Reagent, supplied by HACH. Solution pH was measured with a pH electrode (Basic 20-CRISON).

3. Results and discussion

3.1. Aqueous phase

3.1.1. Chelating agent concentration selection

In order to select an adequate chelating agent concentration, different concentrations of CT were tested in the presence of 882 mol m⁻³ of H₂O₂ and 5 mol m⁻³ of Fe(III), at 293 K. Fig. S1 shows the corresponding H₂O₂ decomposition and CT degradation at different CT concentrations. As can be seen, the conversions of CT are

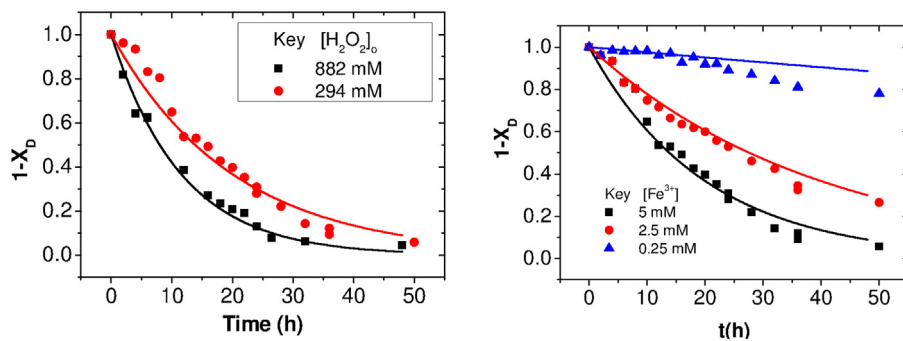


Fig. 1. Remaining diuron oxidation in aqueous phase at different H_2O_2 and $\text{Fe}(\text{III})$ concentrations. $T=293\text{ K}$. (a) at $[\text{CT}]=50\text{ mol m}^{-3}$, $[\text{Fe}(\text{III})]=5\text{ mol m}^{-3}$; (b) at $[\text{CT}]=50\text{ mol m}^{-3}$, $[\text{H}_2\text{O}_2]=294\text{ mol m}^{-3}$.

low at the concentration range analyzed (Fig. S1b). However, as can be seen in Fig. S1a, the decomposition of hydrogen peroxide at the lowest CT concentration used (5 mol m^{-3}) is quite remarkable (50% at 48 h). This could be related to the low pH achieved at this CT concentration ($\text{pH}=2.6$). The lower hydrogen peroxide conversions obtained at higher CT concentrations (12 and 50 mol m^{-3}) can be directly related with the higher pH obtained when CT concentration increases. The higher buffering capacity of the chelating agent at higher concentration is responsible of the neutral pH obtained at 50 mol m^{-3} of CT and, consequently, of the lowest conversion of hydrogen peroxide. Therefore, a CT concentration of 50 mol m^{-3} has been selected to maintain an adequate concentration of dissolved transition metal in near-neutral pH conditions, with low conversions of both the oxidant and the chelating agent in the aqueous phase. Besides, the $\text{Fe}(\text{III})$ concentration remaining in solution, at CT concentration 50 mol m^{-3} , was measured at 50 h, being close to the one initially added (5 mol m^{-3}).

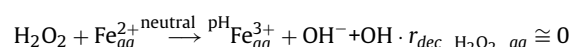
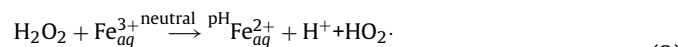
3.1.2. Chelating agent oxidation

The oxidation of CT by H_2O_2 , according to Eq. (1), was analyzed at different experimental conditions. Fig. S2 collects the results of CT oxidation in aqueous phase in the absence and presence of $\text{Fe}(\text{III})$ addition, at different H_2O_2 and CT concentrations. Degradation of CT is almost negligible in absence of iron, even at the highest H_2O_2 concentration used, as can be seen in Fig. S2a. The oxidation of CT in the presence of iron is slightly higher, although the higher degradation (15% at 50 h) is obtained at the lowest CT concentration used (12 mol m^{-3}), as Fig. S2b shows. This could be due, as aforementioned, to the lower pH obtained when lower CT concentrations are used. Besides, an increase of H_2O_2 concentration, at a fixed CT concentration (50 mol m^{-3}), produces only a small increase of the CT oxidation. The CT conversion obtained was 15% at the highest H_2O_2 concentration used. Therefore, the oxidation rate of CT can be considered negligible at these experimental conditions:



3.1.3. Hydrogen peroxide decomposition

Fig. S3 shows the results of H_2O_2 decomposition in the absence and presence of $\text{Fe}(\text{III})$, at the same H_2O_2 and CT concentrations used in Figs. S2a and b. As can be seen, the hydrogen peroxide conversion obtained has been in all cases lower than 10%. Therefore, the decomposition rate of H_2O_2 in the aqueous phase, given in Eq. (2), can be neglected at these experimental conditions.

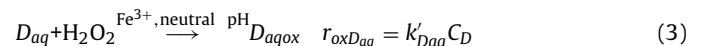


3.1.4. Diuron oxidation

The oxidation of diuron in aqueous phase was evaluated at different H_2O_2 and $\text{Fe}(\text{III})$ concentrations, at 293 K . The corresponding results are shown in Fig. 1a and b. Fig. 1a collects the results of diuron conversion at different H_2O_2 concentrations, with 50 mol m^{-3} of CT and 5 mol m^{-3} of $\text{Fe}(\text{III})$. Fig. 1b shows the remaining diuron at several $\text{Fe}(\text{III})$ concentrations, at 50 mol m^{-3} of CT and 294 mol m^{-3} of H_2O_2 . Neither significant aromatic oxidation intermediates were detected by HPLC in both set of runs.

As can be seen in Fig. 1a, the degradation of diuron in aqueous phase is slightly affected by the H_2O_2 concentrations used. On the other hand, results in Fig. 1b suggest that the aqueous oxidation of diuron is strongly influenced by the catalyst concentration obtaining conversions from 20 to 95%, at 50 h, by using $0.25\text{--}5\text{ mol m}^{-3}$ of $\text{Fe}(\text{III})$.

A first order for diuron concentration has been initially assumed for the oxidation rate of diuron in aqueous phase. Besides, the oxidant and iron cation concentrations do not change with time at the experimental condition used, therefore, a pseudo kinetic constant, k'_D , can be used:



Integration of the mass balance for diuron in a homogeneous batch reactor, taking into account Eq. (3) gives Eq. (4):

$$-\ln(1 - X_{D_{aq}}) = k'_D t \quad (4)$$

being $X_{D_{aq}}$ the diuron conversion in aqueous phase.

Results by applying Eq. (4) are plotted in Fig. 2a and b. As can be seen, an almost linear plot is obtained, confirming the first-order rate law assumed for diuron concentration in Eq. (3). From Fig. 2a, it is deduced that H_2O_2 concentration has a slight effect on the diuron oxidation rate. Results in Fig. 2b indicates that the kinetic constant k'_D increases as iron also does. As the same H_2O_2 concentration was used in all the runs in Fig. 2b, the apparent kinetic constant has been plotted as a function of the corresponding $\text{Fe}(\text{III})$ concentration in Fig. 2c. As can be seen, an almost linear relationship can be obtained between apparent kinetic constant k'_D and iron cation concentration.

Therefore, the apparent kinetic constant has been expressed as a function of the H_2O_2 concentration and the catalyst concentration, according to Eq. (5):

$$k'_D = k_{D_{aq}} \cdot C_{Fe^{3+}} \cdot C_{H_2O_2}^{n_0} \quad (5)$$

From data in Fig. 1a and b and having into account Eqs. (4) and (5), the kinetic constant k_D and the order for H_2O_2 , n_0 , were estimated by using non linear regression, obtaining the following values: $n_0 = 0.5 \pm 0.04$ and $k_D = 5.86 \times 10^{-4} \pm 2.32 \times 10^{-5} \text{ h}^{-1} (\text{mol m}^{-3})^{-1.5}$. Predicted values of remaining diuron in aqueous phase by using Eqs. (4) and (5) are showed as lines in Fig. 1a and b.

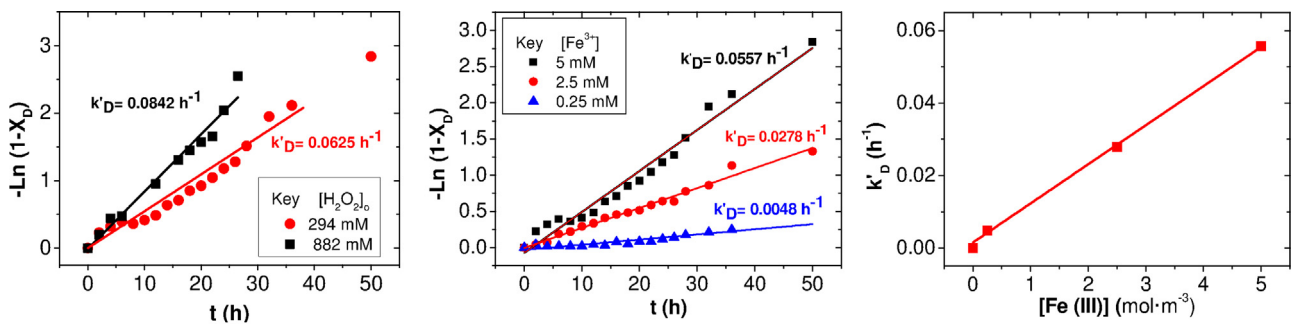


Fig. 2. First-order plot of diuron oxidation rate in aqueous phase according to Eq. (4). (a) Influence of oxidant concentration, $[Fe(III)] = 5 \text{ mol m}^{-3}$, (b) influence of catalyst concentrations $[H_2O_2] = 294 \text{ mol m}^{-3}$, and (c) dependence of the apparent kinetic constant with the catalyst concentration, $[H_2O_2] = 294 \text{ mol m}^{-3}$.

As can be seen a good agreement is found between experimental and simulated values.

3.2. Slurry system

3.2.1. Diuron adsorption-desorption

Sorption equilibrium data of diuron are shown in Fig. 3a, where the adsorbed phase concentration as a function of the aqueous phase concentration is plotted. Equilibrium data were obtained from a contaminated soil with $0.167 \text{ mmol kg}^{-1}$ of diuron, which was maintained in contact with water at different liquid volume to soil mass ratios, for 48 h. Equilibrium was found to be completely reached at this time. The diuron sorption isotherm was fitted to a Freundlich model as follows:

$$q_{De} = K_{FD} \cdot C_{De}^{n_1} \quad (6)$$

The corresponding Freundlich parameters obtained were $2.69 \times 10^{-4} \pm 4.3 \times 10^{-5}$ for K_{FD} (measure of the diuron's sorption capacity) and 0.40 ± 0.05 for n_1 (indicator of the isotherm's curvature).

The influence of chelating agent (at the concentration of 50 mol m^{-3} of CT) was analyzed in both the equilibrium adsorption isotherm and adsorption rate of diuron. Equilibrium values for diuron concentration in soil and aqueous phase were very similar in presence or absence of CT (as can be seen in Fig. 3a), so it seems that the isotherm is not affected by the presence of the chelating agent. On the contrary, the diuron adsorption rate is modified, when CT is added, as it is shown in Fig. 3b, where it can be seen a faster desorption of diuron in the presence of CT than the one observed in the presence of pure water. To describe the kinetic of adsorption rate of diuron, a first order equation for diuron concentration was proposed, but considering that the kinetic adsorption constant is function of the CT concentration, as follows:

Diuron adsorption

$$r_{adsD} = k'_{aD} \cdot (q_{De} - q_D) \quad (7)$$

$$k'_{aD} = k_{aD} \cdot (1 + b \cdot C_{CT}) \quad (8)$$

being q_{De} calculated by means of Eq. (6)

$$r_{adsD} = k_{aD} \cdot (1 + b \cdot C_{CT}) \cdot (K_{FD} \cdot C_{De}^{n_1} - q_D) \quad (9)$$

where r_{adsD} is the adsorption rate of diuron on soil, C_D and C_{CT} are the diuron and CT aqueous phase concentration; q_{Do} , q_D and q_{De} are the initial amount of diuron adsorbed per mass of soil, at any time t and at the equilibrium state, respectively; k'_{aD} and k_{aD} are the apparent and the kinetic rate constants for diuron adsorption; b is an empirical constant, which relates the apparent kinetic rate constant with the CT concentration.

Values in Fig. 3b were fitted to the corresponding mass balance for diuron in the batch slurry system:

$$\frac{dq_D}{dt} = r_{adsD} \quad (10)$$

By using a non-linear regression coupled with an Euler algorithm, data of q_D vs. time shown in Fig. 3b were fitted to Eq. (10), having into account Eqs. (7)–(9). The value of the estimated parameters were $k_{aD} = 0.043 \pm 0.009 \text{ (h}^{-1}\text{)}$ and $b = 0.045 \pm 0.003 \text{ (mol}^{-1} \text{ m}^3\text{)}$.

As can be seen in Fig. 3b, the desorbed diuron amounts simulated by using the above parameters, shown as lines, consistently agree with the experimental ones, for both pure water and a CT concentration of 50 mol m^{-3} .

3.2.2. CT adsorption

The possible adsorption of CT into the soil was also evaluated to quantify the real concentration of CT in the aqueous phase. Fig. 4a shows the CT adsorption isotherm into the soil. The Freundlich equation has been also proposed to fit the equilibrium data of CT adsorption:

$$q_{CTe} = K_{FCT} \cdot C_{CTaq}^{n_2} \quad (11)$$

Values of $2.7 \times 10^{-5} \pm 2.5 \times 10^{-6} \text{ kg}^{-1} \text{ mol}^{-0.2} (\text{m}^3)^{-1.2}$ and 1.20 ± 0.24 , was obtained for the parameters K_{FCT} and n_2 , respectively.

Analyzing the results shown in Fig. 4a, it can be deduced that only a 2–3% of CT is sorbed into the soil when the initial CT concentration is 50 mol m^{-3} . Therefore, the remaining CT concentration in aqueous phase with time can be considered practically constant and equal to the initial value.

3.2.3. Fe extraction by chelating agent

As it is well known, chelating agents can be used to extract the transition metals of the soil. These metals can be also considered as catalysts in the modified Fenton process [11,27]. In previous works, the extraction of naturally occurring metal oxides from soils with some chelating agents was tested. The results showed that chelating agents are able to maintain a considerable amount of Fe in solution [28,29]. In view of these results, the possible extraction of Fe at different CT concentrations and at $V_L \times W^{-1} = 2 \times 10^{-3} \text{ m}^3 \text{ kg}^{-1}$, was also evaluated. Fig. 4b shows the amount of Fe extracted, when equilibrium is reached, as a function of different CT concentrations. The extraction of Fe with only pure water was negligible at these experimental conditions. However, the presence of increasing concentrations of CT produces the extraction of rising concentrations of Fe in the aqueous phase, when equilibrium is reached. These results were adjusted to a power equation, expressed as follows:

$$C_{Feaq} = K_{Fe} \cdot C_{CTaq}^{n_3} \quad (12)$$

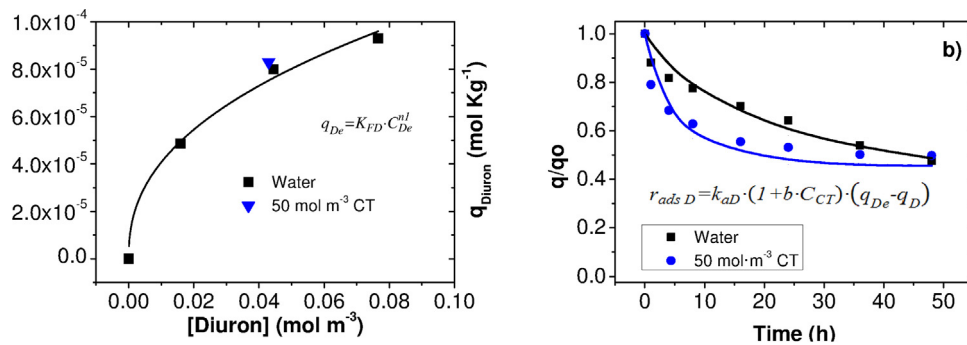


Fig. 3. (a) Adsorption isotherm of diuron on the soil. Symbols: experimental data. Lines: predicted values from Freundlich isotherm. (b) Desorption of diuron from the soil with water or 50 mol m^{-3} of CT, at $V_L \times W^{-1} = 2 \times 10^{-3} \text{ m}^3 \text{ kg}^{-1}$. Symbols: experimental data. Lines: predicted values from the diuron adsorption kinetic model, Eqs. (7)–(10).

The estimated parameters were calculated by fitting the experimental results to this equation, being the estimated values of K_{Fe} and n_3 of $0.0463 \pm 0.0145 (\text{mol m}^{-3})^{0.53}$ and 0.467 ± 0.062 , respectively.

3.2.4. H_2O_2 decomposition

The decomposition of H_2O_2 in the slurry system was evaluated in the presence of 50 mol m^{-3} of CT, at different H_2O_2 concentrations and in the absence or presence of extrinsic Fe(III) addition. Experiments carried out at similar conditions by using contaminated soil with diuron or fresh soil yield the same H_2O_2 conversions, as was previously reported [7,30]. Therefore, the influence of this low contaminant concentration to the H_2O_2 decomposition rate in the slurry system can be ruled out.

This fact is mainly due to the high contribution of the non-productive H_2O_2 reactions due to the presence of both natural organic matter and inorganic species into the soil susceptible of oxidation or catalyzing the H_2O_2 decomposition. Fig. 5a shows the remaining H_2O_2 fraction in the presence of 50 mol m^{-3} of CT at different H_2O_2 concentrations and at $V_L \times W^{-1} = 2 \times 10^{-3} \text{ m}^3 \text{ kg}^{-1}$, without iron added. As can be seen, the conversion profiles of remaining H_2O_2 are very similar at all H_2O_2 concentrations tested, what suggests that the H_2O_2 decomposition is first order with respect to the H_2O_2 concentration. The influence of artificially iron added on the oxidant decomposition is shown in Fig. 5b, at 50 mol m^{-3} of CT, 882 mol m^{-3} of H_2O_2 , and $V_L \times W^{-1} = 2 \times 10^{-3} \text{ m}^3 \text{ kg}^{-1}$. As can be seen, the addition of Fe as catalyst in the aqueous phase did not significantly modify the conversion profiles of H_2O_2 , which is in agreement with the low conversion of H_2O_2 noticed in aqueous phase with or without Fe(III), at neutral pH (Fig. S3). These results confirm that the disappearance of hydrogen peroxide in the slurry system, at the neutral pH used, is mainly due to the unproductive reaction with soil, as was also previously reported [30], with a kinetic constant mainly

depending on the different soil species susceptible of oxidation or acting as a catalyst.

Taking these findings into account, the decomposition rate of H_2O_2 on soil has been expressed as follows:

$$r_{dec, \text{H}_2\text{O}_2, s} = k_{\text{H}_2\text{O}_2} \cdot C_{\text{H}_2\text{O}_2} \quad (13)$$

The mass balance for the H_2O_2 in the slurry system, when only unproductive disappearance of H_2O_2 is considered, can be written as follows:

$$\frac{dn_{\text{H}_2\text{O}_2}}{W \cdot dt} = -k_{\text{H}_2\text{O}_2} \cdot C_{\text{H}_2\text{O}_2} \quad (14)$$

$$\frac{dC_{\text{H}_2\text{O}_2}}{dt} = -k_{\text{H}_2\text{O}_2} \cdot \frac{W}{V_L} \cdot C_{\text{H}_2\text{O}_2} \quad (15)$$

By fitting experimental data in Fig. 5a and b to the integrated Eq. (15), the kinetic constant $k_{\text{H}_2\text{O}_2}$ can be obtained from the slope of the semilogarithmic plot showed in Fig. 5c. A $k_{\text{H}_2\text{O}_2}$ value of $9.68 \times 10^{-5} \pm 4 \times 10^{-6} (\text{m}^3 \text{ kg}^{-1} \text{ h}^{-1})$ was obtained.

3.2.5. Diuron oxidation

Diuron oxidation in slurry system was evaluated at different H_2O_2 concentrations (from 294 to 1765 mol m^{-3}) and the effect of Fe(III) as catalyst was tested. Initial diuron on soil was $0.167 \text{ mmol kg}^{-1}$. CT, as chelating agent, was used at 50 mol m^{-3} . Because of the chelating agent was added 24 h prior to the oxidant addition, the naturally occurring iron oxides from the soil were solubilized and a concentration of Fe(III) in aqueous phase of 0.18 mol m^{-3} was measured (in agreement with results in Fig. 4b). Moreover, equilibrium for desorbed diuron was reached in this period, and the initial concentration of diuron in aqueous and soil phases were 0.048 mol m^{-3} and $7.4 \times 10^{-5} \text{ mol kg}^{-1}$, respectively, before the injection of oxidant. Diuron profiles with time were measured in both aqueous and soil phases, as described in the experimental section. Results are shown in Fig. 6. Normalized concentrations of

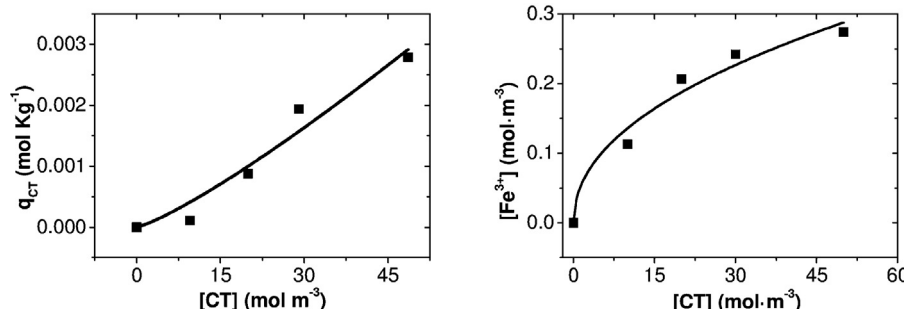


Fig. 4. (a) Adsorption isotherm of CT onto the soil, at $V_L \times W^{-1} = 2 \times 10^{-3} \text{ m}^3 \text{ kg}^{-1}$. Symbols: experimental data. Lines: predicted values with Eq. (11). (b) Influence of CT on Fe(III) extracted in the equilibrium stage. $V_L \times W^{-1} = 2 \times 10^{-3} \text{ m}^3 \text{ kg}^{-1}$. Symbols: experimental data, Lines: predicted value with Eq. (12).

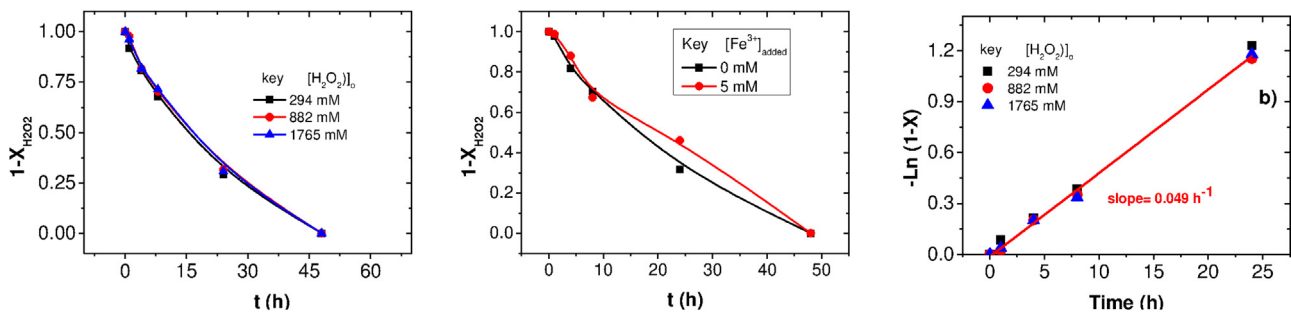


Fig. 5. Remaining oxidant in the slurry system. $[CT] = 50 \text{ mol m}^{-3}$ at $V_L \times W^{-1} = 2 \times 10^{-3} \text{ m}^3 \text{ kg}^{-1}$. (a) Influence of H_2O_2 concentration, (b) influence of $\text{Fe}(\text{III})$ added. $[\text{H}_2\text{O}_2]_0 = 882 \text{ mol m}^{-3}$, (c) first-order plot for H_2O_2 decomposition at several oxidant concentrations, according to Eq. (15).

diuron in aqueous and solid phases are plotted for easier comparison. These normalized concentrations are calculated as the ratio between diuron concentration in a phase at a time t and the diuron concentration in that phase before the oxidant was added. As can be seen in Fig. 6, the diuron oxidation rate increases as the hydrogen peroxide or the catalyst concentration does.

In order to achieve a kinetic model able to predict the diuron conversion in both aqueous and soil phases, different mechanisms have been taken into account for diuron oxidation. One assumption considers that diuron is first desorbed from the soil to the aqueous phase, where the oxidation takes place. The second mechanism takes into account that diuron oxidation takes place in both aqueous and soil phases, at rates r_{oxDag} and r_{oxDs} , respectively. Moreover, diuron sorbed into the soil can be also oxidized by the hydroxyl radicals formed in the aqueous phase or catalyzed by the natural metallic oxides present in soil.

A general mass balance for the oxidant and pollutant in the slurry system is proposed as follows:

Mass balance of H_2O_2

$$\frac{-dC_{\text{H}_2\text{O}_2}}{dt} = r_{\text{dec H}_2\text{O}_2 \text{ aq}} + \frac{W}{V_L} r_{\text{dec H}_2\text{O}_2 \text{ s}} \quad (16)$$

While a negligible oxidant decomposition was found in the aqueous phase ($r_{\text{dec H}_2\text{O}_2 \text{ aq}} \approx 0$), Eq. (16) can be simplified to:

$$\frac{-dC_{\text{H}_2\text{O}_2}}{dt} \approx r_{\text{dec H}_2\text{O}_2 \text{ s}} = \frac{W}{V_L} k_{\text{H}_2\text{O}_2} \cdot C_{\text{H}_2\text{O}_2} \quad (17)$$

Mass balance of diuron (18)

$$\frac{dn_D}{dt} = \frac{dn_{Ds}}{dt} + \frac{dn_{Dag}}{dt} \quad (19)$$

$$\frac{dn_{Ds}}{dt} = r_{\text{adsD}} \cdot W - r_{\text{oxDs}} \cdot W \quad (20)$$

$$\frac{dn_{Dag}}{dt} = -r_{\text{adsD}} \cdot W - r_{\text{oxDag}} \cdot V_L \quad (21)$$

The n_D , n_{Ds} and n_{Dag} are the total moles of diuron in the slurry system, the moles of diuron in soil phase and the moles of diuron in aqueous phase, respectively. Expressions for $r_{\text{dec H}_2\text{O}_2 \text{ s}}$, r_{adsD} and r_{oxDag} are those shown in Eqs. (13), (9) and (3), respectively.

The oxidation rate of sorbed diuron, r_{oxDs} has been proposed to be first order for sorbed diuron concentration. As previously cited, it has been considered that both iron in solution and natural

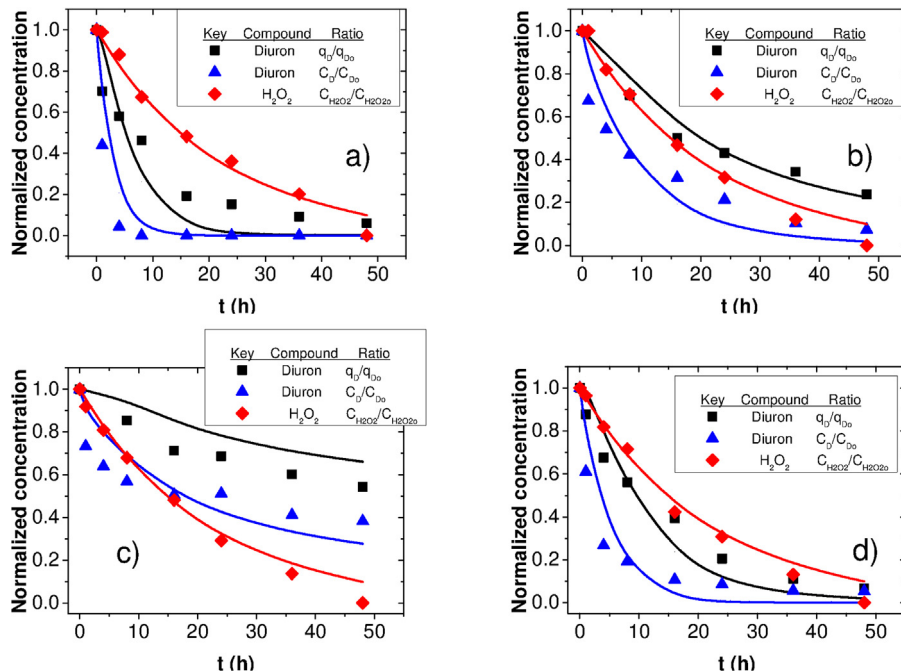


Fig. 6. Normalized concentrations of diuron and H_2O_2 . Symbols: experimental data. Lines: predicted values from Eqs. (17) to (21). Rates summarized in Table 2 and parameter values in Table 3. Initial concentration of diuron in the liquid phase = 0.048 mol m^{-3} ; initial concentration of diuron in the soil phase = $7.4 \times 10^{-5} \text{ mol kg}^{-1}$. $V_L \times W^{-1} = 2 \times 10^{-3} \text{ m}^3 \text{ kg}^{-1}$, $[CT] = 50 \text{ mol m}^{-3}$. (a) $[\text{Fe}^{3+}] = 5 \text{ mol m}^{-3}$, $[\text{H}_2\text{O}_2]_0 = 882 \text{ mol m}^{-3}$; (b) $[\text{Fe}^{3+}] = 0.18 \text{ mol m}^{-3}$, $[\text{H}_2\text{O}_2]_0 = 882 \text{ mol m}^{-3}$; (c) $[\text{Fe}^{3+}] = 0.18 \text{ mol m}^{-3}$, $[\text{H}_2\text{O}_2]_0 = 294 \text{ mol m}^{-3}$; (d) $[\text{Fe}^{3+}] = 0.18 \text{ mol m}^{-3}$, $[\text{H}_2\text{O}_2]_0 = 1786 \text{ mol m}^{-3}$.

Table 2

Reactions taking place in the slurry system and corresponding kinetic equations.

			Units
R1	$CT_{aq} + H_2O_2 \xrightarrow{Fe} CT_{ox}$	$r_{oxCT_{aq}} \approx 0$	–
R2	$H_2O_2 + Fe^{3+}_{aq, neutral} \xrightarrow{pH} Fe^{2+}_{aq} + H^+ + HO_2\cdot$	$r_{desc H_2O_2 aq} \approx 0$	–
	$H_2O_2 + Fe^{2+}_{aq, neutral} \xrightarrow{pH} Fe^{3+}OH^- + OH\cdot$		
R3	$D_{aq} + H_2O_2 \xrightarrow{Fe^{3+}, pH, neutro} D_{aqox}$	$r_{oxD_{aq}} = k_{D_{aq}} C_{Fe^{3+}}^{n_1} C_{H_2O_2}^{n_2} \cdot C_{D_{aq}}$	$mol m^{-3} h^{-1}$
E1	$D_{aq} + S \xrightarrow{k_{oxD_s}} D_{aqox}$	$q_{De} = K_{FD} \cdot C_{De}^{n_1}$	$mmol kg^{-1}$
R4		$r_{adsD} = k_{aD} \cdot (1 + b \cdot C_{CT}) \cdot (q_{De} - q_D)$	$mol kg^{-1} h^{-1}$
E2	$CT_{aq} + soil \leftrightarrow CT_s - soil$	$q_{CTe} = K_{FC_T} \cdot C_{CT_{aq}}^{n_2}$	$mmol kg^{-1}$
E3	$Fe_s + CT_{aq} \leftrightarrow Fe_{aq} + soil$	$C_{Fe_{aque}} = K_{Fe} \cdot C_{CT_{aq}}^{n_2}$	$mmol kg^{-1}$
R5	$H_2O_2 + S \rightarrow S_{ox} + O_2$	$r_{desc H_2O_2 s} = k_{H_2O_2} \cdot C_{H_2O_2}$	$mol kg^{-1} h^{-1}$
R6	$D_s + H_2O_2 \xrightarrow{Fe} D_{sox}$	$r_{oxD_s} = (k_{oxDsh} C_{Fe^{3+}} + k_{oxDsh} C_{H_2O_2}^{n_4}) \cdot q_D$	$mol kg^{-1} h^{-1}$

Table 3

Values of kinetic or equilibrium parameters of the expressions summarized in Table 2.

Parameters obtained in Sections 3.1.1–3.2.4	Estimated parameter. Section 3.3.5. Fitting of data in Fig. 6	CASE 1	CASE 2	CASE 3	CASE 4
$k_{D_{aq}} = 5.86 \times 10^{-4} \pm 2.32 \times 10^{-5} h^{-1} (m^3 mol^{-1})^{1.5}$	k_{aD}	–	$729 \pm 3.66 \times 10^9$	–	$3363 \pm 2.4 \times 10^7$
$n_o = 0.5 \pm 0.04$ (–)	k_{oxDsh}	–	–	$8.08 \times 10^{-4} \pm 4.10 \times 10^{-4}$	$6.53 \times 10^{-4} \pm 2.13 \times 10^{-4}$
$k_{FD} = 2.69 \times 10^{-4} \pm 4.3 \times 10^{-5} kg^{-1} mol^{0.6} (m^3)^{0.4}$	k_{oxDsh}	–	–	$1.18 \times 10^{-4} \pm 0.7 \times 10^{-4}$	$2.36 \times 10^{-4} \pm 0.8 \times 10^{-4}$
$n_1 = 0.40 \pm 0.05$	n_4	–	–	0.79 ± 0.22	0.79 ± 0.1
$k_{aD} = 0.043 \pm 3.13 \times 10^{-3} (h^{-1})$	SQR Total	16.5	16.2	1.90	0.71
$b = 0.045 \pm 0.003 (mol^{-1} m^3)$	SQR aqueous diuron	8.41	8.47	1.63	0.33
$k_{FC_T} = 2.75 \times 10^{-5} \pm 2.5 \times 10^{-6} kg^{-1} mol^{-0.2} (m^3)^{-1.2}$	SQR sorbed diuron	7.93	7.72	0.197	0.29
$n_2 = 1.20 \pm 0.24$	SRQ H_2O_2	0.18	0.08	0.08	0.08
$k_{Fe} = 0.046 \pm 0.014 (mol m^{-3})^{0.53}$	CASE 1: Parameters obtained in Sections 3.1.1–3.2.4 are used to simulate data in Fig. 6 ($k_{oxDs} = 0$). Neither kinetic parameter is estimated	–	–	–	–
$n_3 = 0.47 \pm 0.06$ (–)	CASE 2: Enhanced of adsorption constant due to chemical reaction is included but no oxidation of the diuron sorbed is considered ($k_{oxDs} = 0$)	–	–	–	–
$k_{H_2O_2} = 9.68 \times 10^{-5} \pm 4 \times 10^{-6} (m^3 kg^{-1} h^{-1})$	CASE 3: Oxidation of the diuron sorbed is considered ($k_{oxDs} \neq 0$) but no enhancement of the adsorption constant is supposed	–	–	–	–
	CASE 4: Both enhancement of adsorption constant due to chemical reaction and oxidation of the diuron sorbed ($k_{oxDs} \neq 0$) are considered	–	–	–	–

metallic oxides present in soil could contribute to sorbed diuron oxidation. Besides, a dependence on the H_2O_2 has been taking into account. Therefore, the following expression has been proposed for oxidation rate of sorbed diuron:

$$r_{oxD_s} = (k_{oxDsh} C_{Fe^{3+}} + k_{oxDsh}) C_{H_2O_2}^{n_4} \cdot q_D \quad (22)$$

Table 2 summarizes all the reactions or equilibriums considered in the slurry system and the corresponding kinetic or isotherm expressions proposed. Moreover, at this point, all kinetic or equilibrium parameters but k_{oxDsh} , k_{oxDsH} and n_4 have been calculated in Sections 3.1.1–3.2.4. The estimated values of these parameters are shown at the left column in Table 3.

If the oxidation rate of diuron in the solid phase is neglected ($r_{oxD_s} = 0$), data in Fig. 6 can be predicted by Eqs. (17), (20) and (21) by using the parameters obtained in Sections 3.1.1–3.2.4, and shown at the left column in Table 3 (CASE 1). Sum of square residuals calculated for the normalized H_2O_2 concentration, diuron concentration in both phases and total SQR are also shown in Table 3. As can be seen, SQR values obtained in CASE 1 are quite high, due to the predicted values for remaining diuron were much higher than the experimental ones.

Maintaining the approach of negligible diuron oxidation in the soil phase, an enhancement of the diuron adsorption constant has been assumed (CASE 2), because of the chemical oxidation reaction takes place in the aqueous phase, as reported by Watts et al. [21,22]. Enhanced diuron adsorption constant has been estimated by fitting data in Fig. 6 to Eqs. (17), (20) and (21). As can be seen in Table 3, a higher adsorption constant value is obtained, but only a small decrease of the SQR is achieved. As in CASE 1, predicted values for remaining diuron in both phases were much higher than

experimental ones. Therefore, oxidation reaction in the aqueous phase seems not be the only contribution for diuron disappearance in the media, and oxidation of diuron sorbed onto the soil should be taken into account.

In this sense, the kinetic constants of the oxidation rate of sorbed diuron onto the soil are estimated without considering an enhancement of diuron adsorption constant rate (CASE 3). From fitting data in Fig. 6 to Eqs. (17), (20) and (21), values of k_{oxDsh} and k_{oxDsH} are estimated and summarized in Table 3. As can be seen, a significant lower residual is obtained in CASE 3, in comparison to the calculated

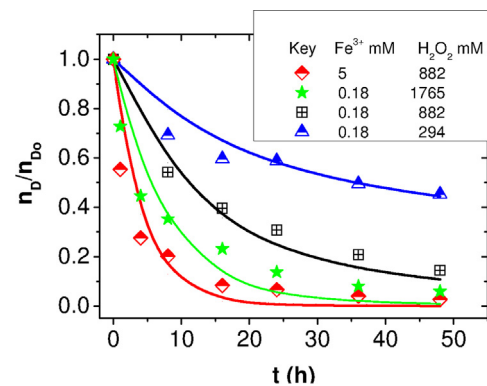


Fig. 7. Total remaining diuron in the slurry system. Symbols: experimental data. Lines: predicted values from Eqs. (17) to (21). Reaction rates summarized in Table 2 and parameter values in Table 3. Initial concentration of diuron in the liquid phase = $0.048 mol m^{-3}$; initial concentration of diuron in the soil phase = $7.4 \times 10^{-5} mol kg^{-1}$. $V_L \times W^{-1} = 2 \times 10^{-3} m^3 kg^{-1}$. Initial total moles of diuron, $n_{D0} = 1.7 \times 10^{-7}$ moles.

in CASES 1 and 2. If an enhancement of the diuron adsorption constant is also included (CASE 4), the estimated values of k_{aD} , k_{oxDsh} and k_{oxDsh} parameters and the SQR are calculated and summarized in Table 3. As shown in this table, the lowest residual is obtained in this CASE 4. Simulated diuron and H₂O₂ profiles for runs shown in Fig. 6, by using Eqs. (17), (20) and (21) with the parameters reported in Table 3 for CASE 4, are plotted as lines. In Fig. 7 the total diuron remaining in the media, experimental data (symbols) and predicted values (lines), is also plotted. As can be observed, simulated and experimental values are very closed, validating the model obtained. It should be noticed that a high value of the enhanced kinetic adsorption constant is estimated in CASES 2 and 4, with a broad confidence interval. This indicates that the adsorption equilibrium is reached quickly, almost instantly, at these conditions.

4. Conclusions

The predicted profiles of diuron, in both soil and aqueous systems, and the oxidant in aqueous phase have been adequately simulated by the kinetic model proposed, that includes the rates of diuron desorption, CT adsorption, H₂O₂ decomposition by soil, and diuron oxidation in the soil and aqueous phases.

The oxidation rate of CT and H₂O₂ can be considered negligible in the aqueous phase if the pH remains at neutral conditions. This neutral pH was here obtained by using a chelating agent with buffer properties. On the other hand, a significant unproductive decomposition of H₂O₂ by the soil takes place under slurry system. Diuron oxidation rate in aqueous phase was strongly dependent of the iron concentration and, in lower extent, of the H₂O₂ concentration. Besides, oxidation of diuron at the soil phase and an enhancement of the diuron kinetic adsorption constant under modified Fenton reaction should be taken into account to predict adequately the experimental results.

Acknowledgements

The authors acknowledge financial support from the Comunidad Autónoma de Madrid provided throughout project CARESOIL (S2009AMB-1648) and from Spanish Ministry of Science and Innovation, project CTM2010-16693.

Appendix A. Supplementary data

Supplementary data associated with this article can be found, in the online version, at <http://dx.doi.org/10.1016/j.apcatb.2013.07.011>.

References

- [1] M.M. Higarashi, W.E. Jardim, *Catal. Today* 76 (2–4) (2002) 201–207.
- [2] S. Giacomazzi, N. Cochet, *Chemosphere* 56 (2004) 1021–1032.
- [3] C.D.S. Tomlin (Ed.), Incorporating the Agrochemicals Handbook, 10th ed., British Crop Protection Council and the Royal Society of Chemistry, Farnham and Cambridge, UK, 1994.
- [4] R.D. Wauchope, T.M. Buttler, A.G. Hornsby, P.W.M. Augustijn-Beckers, *Rev. Environ. Contam. Toxicol.* 123 (1992) 1–157.
- [5] A. Walker, M. Jurado-Exposito, *Weed Res.* 38 (1998) 229–238.
- [6] E. Silva, A.M. Fialho, I. Sá-Correia, R.G. Burns, L.J. Shaw, *Environ. Sci. Technol.* 38 (2004) 632–637.
- [7] F. Vicente, A. Santos, E.G. Saguijo, A.M. Martínez-Villacorta, J.M. Rosas, A. Romero, *Chem. Eng. J.* 170 (2011) 36–43.
- [8] R.D. Villa, R.F. Pupo Nogueira, *Sci. Total Environ.* 371 (2006) 11–18.
- [9] M. Cao, L. Wang, L. Wang, J. Chen, X. Lu, *Chemosphere* (2012), <http://dx.doi.org/10.1016/j.chemosphere.2012.09.098>.
- [10] R.J. Watts, A.L. Teel, *Waste Manage.* 10 (2006) 2–9.
- [11] R.J. Watts, D.D. Finn, L.M. Cutler, J.T. Schmidt, A.L. Teel, *J. Contam. Hydrol.* 91 (2007) 312–326.
- [12] R. Baciocchi, C. Ciotti, G. Cleriti, G. Innocenti, A. Nardella, *J. Adv. Oxid. Technol.* 13 (2010) 153–163.
- [13] C. Lin Yap, S. Gan, H. Kiat Ng, *Chemosphere* 83 (2011) 1414–1430.
- [14] Y. Sun, J.J. Pignatello, *J. Agric. Food Chem.* 40 (1992) 322–327.
- [15] F. Vicente, J.M. Rosas, A. Santos, A. Romero, *Chem. Eng. J.* 172 (2011) 689–697.
- [16] Venny, S. Gan, H.K. Ng, *Chem. Eng. J.* 180 (2012) 1–8.
- [17] S.R. Kanel, B. Neppolian, H. Choi, J.W. Yang, *Soil Sediment. Contam.* 12 (2003) 101–117.
- [18] J.J. Pignatello, E. Oliveros, A. Mackay, *Crit. Rev. Env. Sci. Technol.* 36 (2006) 1–84.
- [19] E. Neyens, J. Baeyens, *J. Hazard. Mater.* 98 (2003) 33–50.
- [20] F.J. Rivas, *J. Hazard. Mater.* B138 (2006) 234–251.
- [21] R.J. Watts, P.C. Stanton, J. Howsawkg, A.M. Teel, *Water Res.* 36 (2002) 4283–4292.
- [22] R.J. Watts, B.C. Bottenberg, T.F. Hess, M.D. Jensen, A.L. Teel, *Environ. Sci. Technol.* 33 (1999) 3432–3437.
- [23] W.P. Kwan, B.M. Voelker, *Environ. Sci. Technol.* 37 (2003) 1150–1158.
- [24] S.R. Kanel, B. Neppolian, H. Jung, H. Choi, *Environ. Eng. Sci.* 21 (2004) 741–751.
- [25] NEN 5754 Method. (1994) Determination of organic matter content in soil as loss.on-ignition.
- [26] USEPA 3050B Method. (1996) Acid digestion of sediments, sludges and soils.
- [27] A. Rastogi, S.R. Al-Abed, D.D. Dionysiou, *Appl. Catal. B: Environ.* 85 (2009) 171–179.
- [28] X. Xu, R.X. Thomson, *Chemosphere* 69 (2007) 755–762.
- [29] J.M. Rosas, F. Vicente, A. Santos, A. Romero, *Chem. Eng. J.* 220 (2013) 125–132.
- [30] A. Romero, A. Santos, T. Cordero, J. Rodriguez-Mirasol, J.M. Rosas, F. Vicente, *Chem. Eng. J.* 170 (2011) 36–43.